Available online at www.sciencedirect.com
ScienceDirect
Comput. Methods Appl. Mech. Engrg. 196 (2007) 5084–5091
Computer methods in applied mechanics and engineering
www.elsevier.com/locate/cma

Optimal shape determination of a body located in incompressible viscous fluid flow

Hiroko Yagi, Mutsuto Kawahara *

Department of Civil Engineering, Chuo University, Kasuga 1-13-27, Bunkyo-ku, Tokyo 112-8551, Japan

Received 15 March 2007; received in revised form 6 July 2007; accepted 17 July 2007
Available online 28 July 2007

Abstract

The purpose of this study is to present a formulation and numerical results of a shape optimization of a body located in the incompressible viscous flow field. The formulation is based on an optimal control theory in which a performance function of fluid forces is introduced. The performance function should be minimized satisfying the state equation. Based on the adjoint equation, the gradient of the performance function can be derived. The weighted gradient method is successfully utilized as the minimization algorithm. The bubble function finite element method originated by authors' group is used for the spatial discretization. For the control variables, the coordinate of the body is employed. The Delaunay triangulation is employed for the discretization with smoothing technique for the gradient. At the moderate Reynolds number flow, the drag minimization of a wing shape body located in the unsteady Navier–Stokes flow is carried out. Starting from a circular cylinder, the streamline shape has been obtained, which is similar to the NACA wing shape. However, the shape shows front-edged and rear-round type. It is clarified that the Reynolds number $Re = 250$ flow corresponds to the critical state at which the minimum drag force shape changes from the front-edge shape to the front-round shape.

Keywords: Optimal shape; Optimal control theory; Finite element method; Navier–Stokes equation; Mixed interpolation; Weighted gradient method; Fluid force; Streamline shape

1. Introduction

A shape optimization is important for the design of airplane wing, airplane body, motor car, high-speed train, racing yacht, etc. To determine shapes of those bodies, the drag minimization or lift maximization are one of the main design procedures. In the numerical determination, the shape optimization problem can be transformed into the minimization problem without constraint condition by the Lagrange multiplier and the adjoint equations using adjoint variables corresponding to the state equation.

Academic work of the shape optimization is presented by Pironneau [1,2]. He investigated that the method of shape optimality using the gradient is determined by taking variation with respect to a coordinate of the body. He et al. [3] shows the method based on the Bezier curves. Kawahara and his group [4,7,11,12] investigated the body shape in the Navier–Stokes flow by the finite element method based on the optimal control theory. They have pointed out that the front-edge and rear-round shape of the streamline shape is the minimum drag body shape. Mohamadi and Pironneau [8] published the book about shape optimizations for fluid, in which they treated with almost time independent problem. Jameson [9] delivered the presentation at Von Karman Institute that practical airplane wing is designed using the adjoint method. The research by Katamine et al. [13] is concerned with the traction method for the optimization.

In the shape optimization, the most important is the performance function. For a airplane wing, the drag force should be minimized but the lift force should retain the

* Corresponding author. Tel.: +81 3 3817 1811; fax: +81 3 3817 1803.
E-mail address: kawa@civil.chuo-u.ac.jp (M. Kawahara).

0045-7825/$ - see front matter © 2007 Elsevier B.V. All rights reserved.
doi:10.1016/j.cma.2007.07.008

value to support the airplane weight. Contrary to this, for a racing car or high-speed train, the minimization of both drag and lift forces are required. For some other problems, only the drag force is the design variable. Jameson [9] treated with the pressure on the wing as the performance function. As the design variables, He et al. [3] employed Bezier function. The finite element mesh used for the computation is important. Basically, non-structured mesh is used, but in this case, the smoothing should be introduced because the calculated gradient should be smoothed. To obtain the gradient for the minimization, there are direct formulation, indirect formulation, AD formulation and others.

In the present paper, the formulation is based on the transient incompressible Navier–Stokes equation. The drag force minimization is treated using the weighted gradient method because from the wide range of the starting configuration, the stable computation can be secured. The coordinates to define the body shape are taken as the design variables. The gradient for the optimization of the performance function can be directly obtained by the first variation of the extended performance function. The bubble function interpolation originated by Kawahara and his group [5,6], is usefully utilized. To obtained the smooth gradient on the body the smoothing technique of Jameson [9,10] is used. At the moderate Reynolds number flow ($Re = 250$), the numerical computation has been performed using a NACA shape starting from a circular cylinder. The streamline shape can be obtained at the final stage. At low Reynolds number flow lower than 250, front-edged and rear-round shape is computed. In the case that the Reynolds number is higher than 250, front-round and rear-edged shape is obtained. Thus, the flow of Reynolds number $Re = 250$ seems to be the critical state. The computation is precisely performed near the critical point. The experience gained in this paper is useful not only in the sense of academic work but also practical work.

2. State equation

2.1. Navier–Stokes equation

The formulation of shape optimization is based on an optimal control theory. In this paper, indicial notation and the summation convection with repeated indices are used to describe equation. Consider a typical problem shown in Fig. 1, in which a solid body B with the boundary Γ_B is laid in an external flow. Let Γ denote the boundary of Ω and suppose that an incompressible viscous flow occupies Ω. The state equation of the flow can be written by the Navier–Stokes equation in the non-dimensional form,

$$\dot{u}_i + u_j u_{i,j} + p_{,i} - \nu(u_{i,j} + u_{j,i})_{,j} = 0 \quad \text{in } \Omega, \tag{1}$$

$$u_{i,i} = 0 \quad \text{in } \Omega, \tag{2}$$

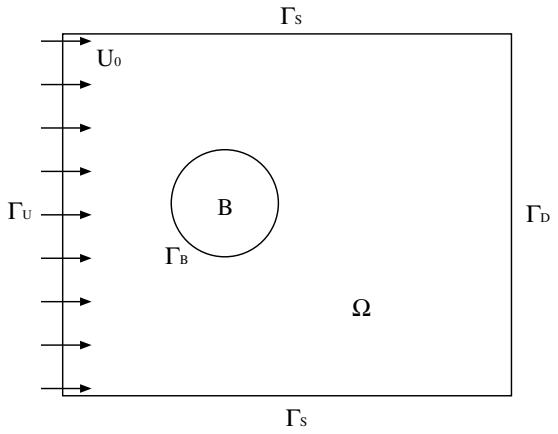

Fig. 1. Computational domain and boundary condition.

where, u_i, p and ν are velocity, pressure, and the viscosity coefficient ($\nu = 1/Re$) respectively, in which Re is the Reynolds number.

Suppose that the boundary conditions are as follows:

$$u_i = \hat{u}_i \quad \text{on } \Gamma_U, \tag{3}$$

$$t_1 = 0, \quad u_2 = 0 \quad \text{on } \Gamma_S, \tag{4}$$

$$u_i = 0 \quad \text{on } \Gamma_B, \tag{5}$$

$$t_i = 0 \quad \text{on } \Gamma_D, \tag{6}$$

where,

$$t_i = \{-p\delta_{ij} + \nu(u_{i,j} + u_{j,i})\}n_j, \tag{7}$$

in which t_i is traction, and n_j is a unit vector of outward normal to Γ, respectively.

The fluid forces subjected to the body are denoted by F_i, where F_1 and F_2 are drag and lift forces, respectively. The fluid force F_i is obtained integrating the traction t_i on the boundary Γ_B as

$$F_i = -\int_{\Gamma_B} t_i \mathrm{d}\Gamma. \tag{8}$$

2.2. Mixed interpolation

The weighted residual equation of the basic equation is written as follows:

$$\int_\Omega w_i \dot{u}_i \mathrm{d}\Omega + \int_\Omega w_i u_j u_{i,j} d\Omega + \int_\Omega w_{i,j}\{-p\delta_{ij} + \nu(u_{i,j} + u_{j,i})\}\mathrm{d}\Omega = \int_\Gamma w_i t_i \mathrm{d}\Gamma, \tag{9}$$

$$\int_\Omega q u_{i,i} \mathrm{d}\Omega = 0. \tag{10}$$

As for the spatial discretization of the bubble function interpolation presented by the author's group (Matsumoto et al. [5], Matsumoto and Kawahara [6]), the mixed interpolation

for the momentum and pressure equations can be expressed as:

(a) bubble function interpolation for velocity

$$u_i = \Phi_1 u_{i1} + \Phi_2 u_{i2} + \Phi_3 u_{i3} + \Phi_4 \tilde{u}_{i4},$$
$$\tilde{u}_{i4} = u_{i4} - \frac{1}{3}(u_{i1} + u_{i2} + u_{i3}),$$
$$\Phi_1 = \eta_1, \quad \Phi_2 = \eta_2, \quad \Phi_3 = \eta_3, \quad \Phi_4 = 27\eta_1\eta_2\eta_3, \tag{11}$$

and

(b) linear interpolation for pressure

$$p = \Psi_1 p_1 + \Psi_2 p_2 + \Psi_3 p_3,$$
$$\Psi_1 = \eta_1, \quad \Psi_2 = \eta_2, \quad \Psi_3 = \eta_3, \tag{12}$$

where $\Phi_\alpha (\alpha = 1, 4)$ is the bubble function in four-node triangular element, $\Psi_\lambda (\lambda = 1, 3)$ is the linear interpolation for pressure in three-node triangular element in which η_1, η_2 and η_3 are area coordinate and $u_{i\alpha}$ and p_λ represent the nodal values at the αth node of each finite element, respectively as shown in Fig. 2.

The criteria for the steady problem is used, in which the discretized form derived by the bubble function interpolation is equivalent to those by the SUPG method [4]. In the bubble function element for the steady problem, the stabilized parameter τ_{eB} which determines the magnitude of the streamline stabilized term can be given by:

$$\tau_{eB} = \frac{\langle \phi_e, 1 \rangle^2_{\Omega_e}}{v \| \phi_{e,j} \|^2_{\Omega_e} A_e}, \tag{13}$$

where $\langle u', v' \rangle_{\Omega_e} = \int_{\Omega_e} u'v' \mathrm{d}\Omega$, $\|u'\|^2_{\Omega_e} = \int_{\Omega_e} u'u' \mathrm{d}\Omega$ and $A_e = \int_{\Omega_e} \mathrm{d}\Omega$, respectively. From the criteria for the stabilized parameter in the SUPG method, an optimal parameter τ_{eS} can be chosen as:

$$\tau_{eS} = \left[\left(\frac{2|u'_i|}{h_e} \right)^2 + \left(\frac{4v}{h_e^2} \right)^2 \right]^{-\frac{1}{2}}, \tag{14}$$

where h_e is an element size.

Generally (13) is not equal to (14). The bubble function that gives optimal viscosity satisfies the following equation expressed by the stabilized operator control parameter v:

$$\frac{\langle \phi_e, 1 \rangle^2_{\Omega_e}}{v \| \phi_{e,j} \|^2_{\Omega_e} A_e} = \tau_{eS}, \tag{15}$$

It is shown that (15) adds stabilized operator control term (16) only of the barycenter point concerned with the equation of motion:

$$\sum_{e=1}^{N_e} v' \| \phi_{e,j} \|^2_{\Omega_e} b_e, \tag{16}$$

where N_e and b_e are the total number of elements and the bubble degree of freedom.

2.3. Finite element equation

The finite element equation can be described as follows:

$$M\dot{U}_i + A_{\alpha\beta\gamma,j}(U_j)U_i - C_{\alpha,i\beta}P + D_{\alpha,j\beta,j}U_i + D_{\alpha,j\beta,i}U_j = T_i \quad \text{in } \Omega, \tag{17}$$

$$C^T_{\alpha,i\beta}U_i = 0 \quad \text{in } \Omega, \tag{18}$$

where,

$$M = \int_\Omega N_\alpha N_\beta \mathrm{d}\Omega, \quad D_{\alpha,j\beta,i} = v \int_\Omega N_{\alpha,j} N_{\beta,i} \mathrm{d}\Omega,$$
$$T_i = \int_{\Gamma_B} \eta t^h_i \mathrm{d}\Gamma, \quad A_{\alpha\beta\gamma,i}(U_i) = \int_\Omega N_\alpha N_\beta U_i N_{\gamma,i} \mathrm{d}\Omega,$$
$$C_{\alpha,i\beta} = \int_\Omega N_{\alpha,i} N_\beta \mathrm{d}\Omega,$$

where N and η are the interpolation function for each element of domain and boundary, respectively. The approximated trial function of the velocity and pressure are denoted by U_i and P, respectively.

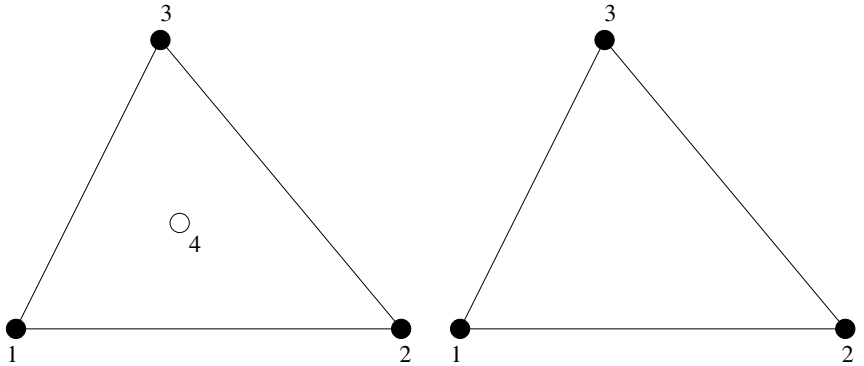

(a) Bubble function Element (b) Linear Element

Fig. 2. Mixed interpolation function.

3. Shape determination

In this research, the shape is defined using n design parameter $X_1, X_2, \ldots, X_n$. which express the coordinate of the surface of the body minimizing the fluid forces subjected to the body under the constraints of the Navier–Stokes equations.

3.1. Volume constraint

The shape of the body should be optimized keeping the volume constant. The volume is being kept in each iteration cycle. To keep the volume of the body is equal to keep the volume of the whole computational domain. The volume constraint function yields as follows,

$$\sum_{e=1}^{m}(a_e(X_i)) - A_0 = 0, \tag{19}$$

where $a_e(X_i)$ is the volume of each element[1] and A_0 is the volume of the initial whole domain.

3.2. Performance function

In this paper, a fluid force control problem is treated. The performance function J is defined by the square sum of the residual between values of computed fluid and objective fluid forces as:

$$J = \frac{1}{2}\int_{t_0}^{t_f}\left(q_1F_1^2 + q_2F_2^2\right)\mathrm{d}t, \tag{20}$$

where q_1 and q_2 are the weighting parameters of the drag and lift forces, respectively. The performance function should be minimized satisfying (17) and (18). The Lagrange multiplier method is suitable for the optimal control problem with the constraint conditions. The Lagrange multipliers for (17) and (18) and volume constraint are defined as adjoint velocity U_i^*, adjoint pressure P^* and adjoint variable λ, respectively. The problem can be transformed into the stationary problem of the extended performance function J^*.

$$\begin{aligned} J^* = {} & \frac{1}{2}\int_{t_0}^{t_f}\left(q_1F_1^2 + q_2F_2^2\right)\mathrm{d}t - \int_{t_0}^{t_f} U_i^{*T}\left(M\dot{U}_i + A_{\alpha\beta\gamma,j}(U_j)U_i\right. \\ & \left. - C_{\alpha,i\beta}P + D_{\alpha,j\beta,j}U_i + D_{\alpha,j\beta,i}U_j - T_i\right)\mathrm{d}t \\ & + \int_{t_0}^{t_f} P^{*T}C_{\alpha,i\beta}^{T}U_i\mathrm{d}t + \lambda\left\{\sum_{e=1}^{m}(a_e(X_i)) - A_0\right\}, \end{aligned} \tag{21}$$

where discretized velocity and pressure are denoted by U_i and P, respectively.[2]

3.3. Stationary condition

The optimal control problem with constraint condition of (17) and (18) results in solving a stationary condition of the extended performance function J^* instead of the original performance function J. The stationary condition of the extended performance function J^* can be derived from the first variation:

$$\begin{aligned} \delta J^* = {} & -\int_{t_0}^{t_f}\delta U_i^{*}\mathrm{T}\left(M\dot{U}_i + A_{\alpha\beta\gamma,j}(U_j)U_i - C_{\alpha,i\beta}P\right. \\ & \left. + D_{\alpha,j\beta,j}U_i + D_{\alpha,j\beta,i}U_j - T_i\right)\mathrm{d}t + \int_{t_0}^{t_f}\delta P^{*}\mathrm{T}C_{\alpha,i\beta}^{\mathrm{T}}U_i\mathrm{d}t \\ & - \int_{t_0}^{t_f}\delta U_i^{\mathrm{T}}\left(-M^{\mathrm{T}}\dot{U}_i^{*} + A_{\alpha\beta\gamma,j}^{\mathrm{T}}(U_j)U_i^{*} - C_{\alpha,i\beta}P^{*}\right. \\ & \left. + D_{\alpha,j\beta,j}^{\mathrm{T}}U_i^{*} + D_{\alpha,i\beta,j}^{\mathrm{T}}U_j^{*}\right)\mathrm{d}t + \int_{t_0}^{t_f}\delta P^{\mathrm{T}}C_{\alpha,i\beta}^{\mathrm{T}}U_i^{*}\mathrm{d}t \\ & + \int_{t_0}^{t_f}\delta T_i^{\mathrm{T}}\left(U_i^{*} - q_iF_i\right)\mathrm{d}t + \delta\lambda^{\mathrm{T}}\{\sum_{e=1}^{m}(a_e(X_i)) - A_0\} \\ & + \delta X_i^{\mathrm{T}}G_i - U_i^{*\mathrm{T}}(t_f)M\delta U(t_f) + U_i^{*\mathrm{T}}(t_0)M\delta U(t_0), \end{aligned} \tag{22}$$

where

$$\begin{aligned} G_k = {} & -\int_{t_0}^{t_f} U_i^{*\mathrm{T}}\left(\frac{\partial M}{\partial X_k}\dot{U}_i + \frac{\partial A_{\alpha\beta\gamma,j}(U_j)}{\partial X_k}U_i - \frac{\partial C_{\alpha,i\beta}}{\partial X_k}P\right. \\ & \left. + \frac{\partial D_{\alpha,j\beta,j}}{\partial X_k}U_i + \frac{\partial D_{\alpha,j\beta,i}}{\partial X_k}U_j - \frac{\partial T_i}{\partial X_k}\right)\mathrm{d}t \\ & + \int_{t_0}^{t_f} P^{*\mathrm{T}}\frac{\partial C_{\alpha,i\beta}^{\mathrm{T}}}{\partial X_k}U_i\mathrm{d}t + \lambda^{\mathrm{T}}\frac{\partial}{\partial X_k}\sum_{e=1}^{m}a_e(X_i), \end{aligned} \tag{23}$$

in which G_k gives the gradient of the extended performance function and X_i is the coordinate on the surface of the body. Setting each term equal to zero to satisfy the optimal condition, the following conditions are derived.

$$\begin{aligned} & M\dot{U}_i + A_{\alpha\beta,j}(U_j)U_i - C_{\alpha,i\beta}P + D_{\alpha,j\beta,j}U_i \\ & \quad + D_{\alpha,j\beta,i}U_j = T_i \quad \text{in } \Omega, \end{aligned} \tag{24}$$

$$C_{\alpha,i\beta}^{\mathrm{T}}U_i = 0 \quad \text{in } \Omega, \tag{25}$$

$$U_i(t_0) = \widehat{U}_i(t_0) \quad \text{in } \Omega, \tag{26}$$

$$\begin{aligned} & -M^{\mathrm{T}}\dot{U}_i^{*} + A_{\alpha\beta,j}^{\mathrm{T}}(U_j)U_i^{*} - C_{\alpha,i\beta}P^{*} \\ & \quad + D_{\alpha,j\beta,j}^{\mathrm{T}}U_i^{*} + D_{\alpha,j\beta,i}^{\mathrm{T}}U_j^{*} = T_i^{*} \text{ in } \quad \Omega, \end{aligned} \tag{27}$$

$$C_{\alpha,i\beta}^{\mathrm{T}}U_i^{*} = 0 \quad \text{in } \Omega, \tag{28}$$

[1] In the shape optimization problem, the volume of each element is the function of the coordinate on the target body X_i. Because the volume of each element is updated at the each iteration. In this study, the shape optimization problem discusses by using the discretized state equation. Therefore, the volume of each element is expressed by $a_e(X_i)$.

[2] The discretized adjoint equation in space is directly obtained by using the discretized state equation including the stabilization term as the constraint condition for the performance function. In addition, the derived adjoint equation is included the stabilization term equivalent to that term in the state equation.

$$U_i^*(t_f) = 0 \quad \text{in } \Omega, \tag{29}$$

$$q_i F_i - U_i^* = 0 \quad \text{on } \Gamma_B, \tag{30}$$

$$\sum_{e=1}^{m}(a_e(X_i)) - A_0 = 0 \quad \text{in } \Omega, \tag{31}$$

$$G_i = 0 \quad \text{in } \Omega, \tag{32}$$

where T_i^* means the traction vector for adjoint variables given by the gradient of the extended performance function with respect to the velocity. Finally, considering the boundary condition for state variables (3)–(6), the boundary condition for adjoint variables can be derived as

$$u_i^* = 0 \quad \text{on } \Gamma_U, \tag{33}$$

$$t_1^* = 0, \quad u_2^* = 0 \quad \text{on } \Gamma_S, \tag{34}$$

$$u_i^* = q_i F_i \quad \text{on } \Gamma_B, \tag{35}$$

$$t_i^* = 0 \quad \text{on } \Gamma_D, \tag{36}$$

where (35) can be obtained by (30). If U_i, P, U_i^*, P^*, and λ are solved satisfying (24) to (32), the optimal condition of this problem is given by (37) as follows:

$$\frac{\partial J^*}{\partial X_i} = G_i = 0. \tag{37}$$

3.4. Smoothing

It is known from the previous research (12) that the computed gradient depends on the irregularity of the mesh. In addition, numerical oscillation is significant. Therefore, in this research, the gradient is smoothed using the smoothing equation (10). The computed gradient G can be smoothed as follows:

$$\overline{G} - \epsilon\frac{\partial^2 \overline{G}}{\partial \xi^2} = G, \tag{38}$$

where $\overline{G}$ denotes the modified gradient and ϵ denotes the arbitrary parameter which is used to adjust the smoothness. If the second-order central differencing is applied to (38), the equation can be expressed as

$$\overline{G}_i - \epsilon\left(\overline{G}_{i+1} - 2\overline{G}_i + \overline{G}_{i-1}\right) = G_i. \tag{39}$$

Assembling the each elements on the target body, the equation can be written as follows.

$$A\overline{G} = G. \tag{40}$$

where A is the $n \times n$ tri-diagonal matrix. Finally, the modified gradient $\overline{G}_i$ can be computed by following equation.

$$\overline{G} = A^{-1}G. \tag{41}$$

3.5. Weighted gradient method

As the minimization technique, the weighted gradient method, which seems to be scarcely dependent on the initial value, is applied. In this method, a modified performance function, $K^{(l)}$, which is obtained adding a penalty term to the extended performance function, is introduced. Let $X_i^{(l)}$ be design variable at (l)th iteration, the modified performance function is expressed as follows:

$$K^{(l)} = J^{*(l)} + \frac{1}{2}\left(X_i^{(l+1)} - X_i^{(l)}\right)^{\mathrm{T}} W\left(X_i^{(l+1)} - X_i^{(l)}\right), \tag{42}$$

where l is iteration number of minimization and W is weighting parameter, respectively. The convergence rate can be controlled by the weighting parameter W. In case that the modified performance function converges to the minimum, the penalty term can also be zero, i.e., minimization of the modified performance function is equal to the minimization of the extended performance function.

$$\delta K^{(l)} = \frac{\partial J^{*(l)}}{\partial X_i}\delta X_i^{(l)} + W\left(X_i^{(l+1)} - X_i^{(l)}\right)\delta X_i^{(l)}. \tag{43}$$

From the stationary condition:

$$\delta K^{(l)} = 0. \tag{44}$$

the equation used for the renewal of shape in each iteration cycle is obtained as follows:

$$X_i^{(l+1)} = X_i^{(l)} - \frac{1}{W}\frac{\partial J^{*(l)}}{\partial X_i} = X_i^{(l)} - \frac{1}{W}G_i^{(l)} \tag{45}$$

3.6. Algorithm

The following algorithm can be introduced.

(1) Select initial surface coordinates $X_i^{(0)}$ in Ω.
(2) Solve $u_i^{(0)}$, $p^{(0)}$ by Eqs. (24) and (25) under the initial condition (26) and the boundary conditions (3)–(6) in Ω.
(3) Compute $J^{(0)}$.
(4) Solve $u_i^{*(0)}$, $p^{*(0)}$ by Eqs. (27) and (28) under the terminal condition (29) and the boundary conditions (33)–(36) in Ω.
(5) Compute the modified gradient $\overline{G}$ by Eq. (41).
(6) Compute $X_i^{(k)}$ by Eq. (45) using the modified gradient $\overline{G}$ instead of the computed gradient G.
(7) Solve $u_i^{(k)}$, $p^{(k)}$ by Eqs. (24) and (25) in Ω.
(8) Compute $J^{(k)}$.
(9) If $|X_i^{(k)} - X_i^{(k-1)}| < \varepsilon$ then stop, else solve $u_i^{*(k)}$, $p^{*(k)}$ by Eqs. (27) and (28) under the terminal condition (29) and the boundary conditions (33)–(36) in Ω, go to (5).

4. Numerical study

The shape optimization of a body located in the incompressible viscous flow is performed. The Reynolds number is 250.0. As an initial shape, a circular cylinder is introduced. Figs. 3 and 4 show the computational domain and finite element mesh. The Delaunay type mesh triangulation is used.

As the control variable, nodal coordinates of the body are used. The gradient is computed based on the direct

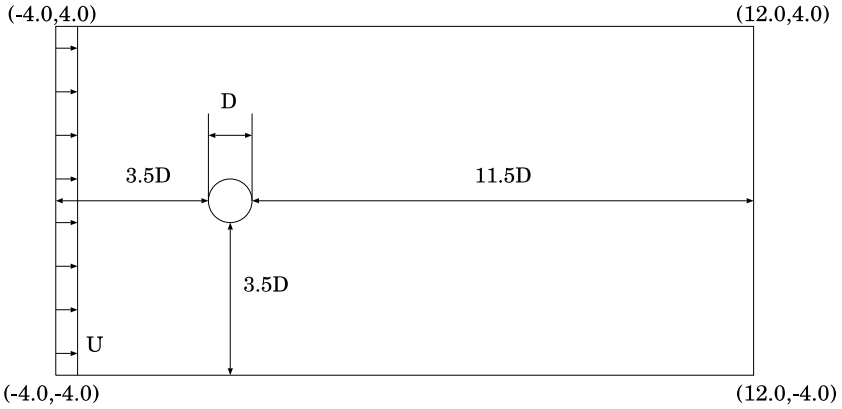

Fig. 3. Computational domain.

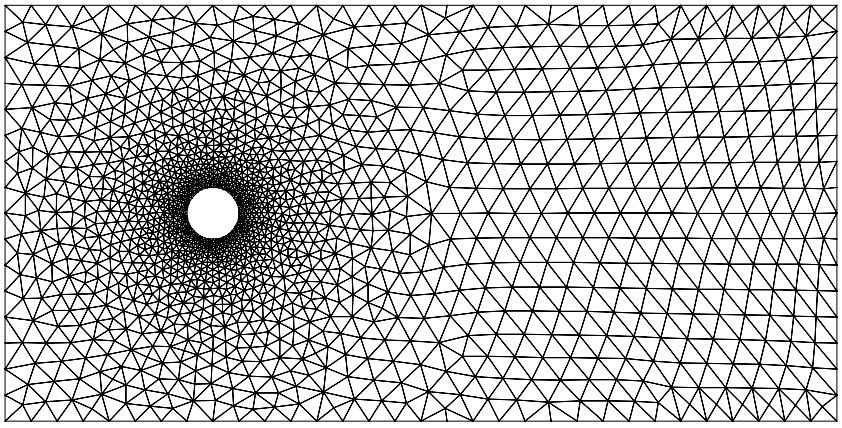

Fig. 4. Finite element mesh.

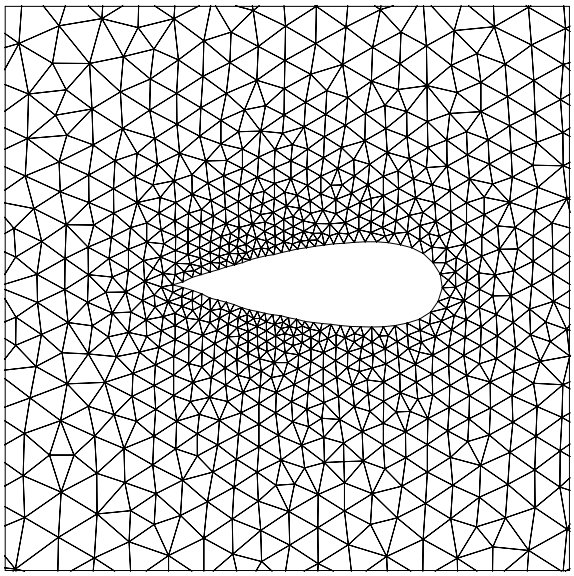

Fig. 5. Finite element mesh.

sensitivity calculation. Fig. 5 represents the final shape of the computation.[3] The shape is converged to the thinner configuration and the center of gravity is moved to back side as shown in Fig. 5. The drag force is reduced to 65% of the initial stage. In this computation, the values of the gradient obtained around the body are not smooth. Thus, the smoothing should be employed. Fig. 6 shows the pressure and stream line of the initial and final cylinders, respectively. The final configuration in Fig. 6b represents that the pressure is reduced and the stream line becomes close to the straight line.

The final shape of the cylinder obtained is the front-edged and rear-round type shape, which seems the inverse position to the streamline shape. To clarify the obtained final shape, the following computations have been carried out. The drag force of the cylinders have computed changing the shapes from NACA0090 to NACA0005 as shown in Fig. 7.[4] Each volume is the same as the initial circular cylinder. Moreover, these shapes are laid in two types of positions, i.e., normal and inverse positions, as shown in Fig. 8.

The drag force at each configuration has computed and plotted in Fig. 9, which shows the non-dimensional drag force.[5] Looking in Fig. 9 and its amplified figure, Fig. 10,

[3] It takes 80 iterations to obtain the final shape.

[4] These data can be obtained on the web page <http://www.pagend-arm.de/trapp/programming/java/profiles/NACA4.htm>.

[5] In Fig. 9, the thickness ratio is calculated based on the diameter of the cylinder D and means the ratio between the thickness of the NACA airfoil series and the diameter of the cylinder.

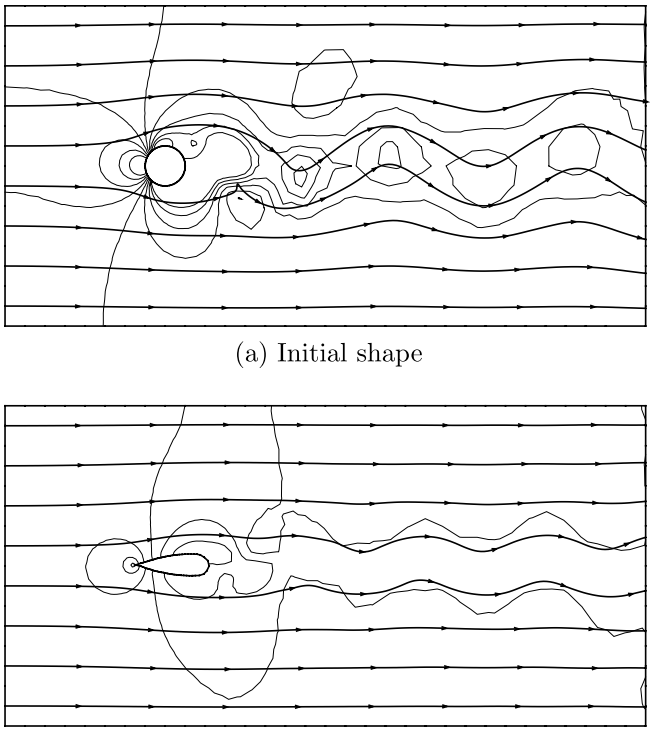

(a) Initial shape

(b) Final shape

Fig. 6. (a) Initial shape and (b) final shape pressure contour and stream line distribution.

the variation of the drag force at each shape can be clarified. At the point of thickness ratio, 40 and above, the drag force at the inverse position is smaller than that at the normal position. Contrary to this, at the point of thickness ratio, 40 and the less, the drag force at the normal position is smaller than that at the inverse position. Namely, thickness ratio is more than 40, the drag force of the front-round and rear-edged type shape is smaller than that of the front-edged and rear-round type shape. However, the thickness ratio is less than 40, the drag force of the front-edge shape is smaller than the front-round type shape. The drag force at the final shape obtained by the present computation is also plotted in Fig. 9. The final shape computed shows that the drag force is reduced by 66.5%. The drag force of the optimal shape of the front-edge and rear-round shape, which is normal streamline shape, is reduced by 66.8%. Those are the computed results at Reynolds number 250, i.e., the moderate Reynolds number flow. The numerical computation at lower Reynolds number flows illustrates that the final shape is all front-edged and rear-round type shape.

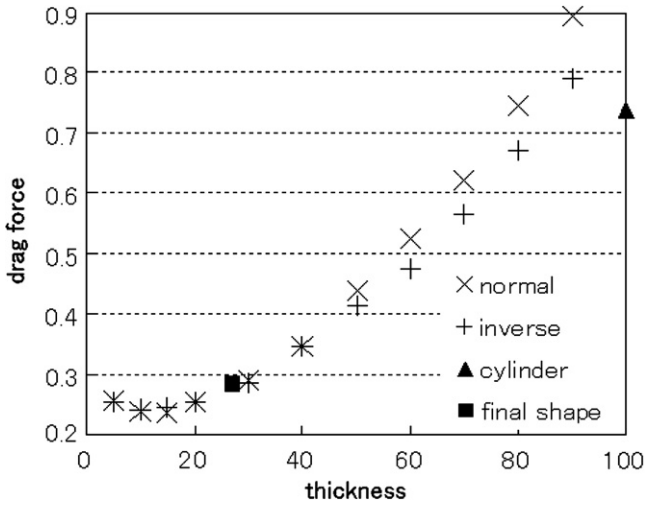

Fig. 9. Drag forces.

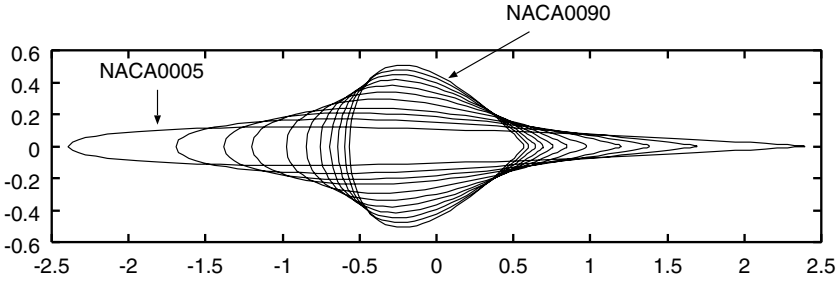

Fig. 7. NACA4 airfoil series.

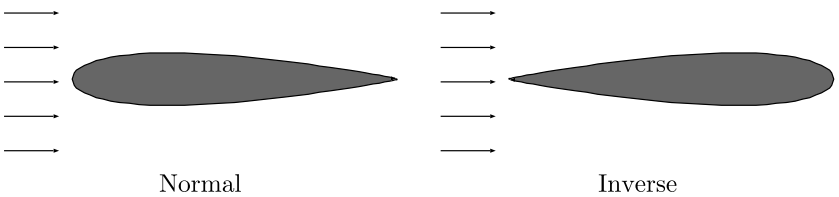

Fig. 8. Two positions (normal and inverse).

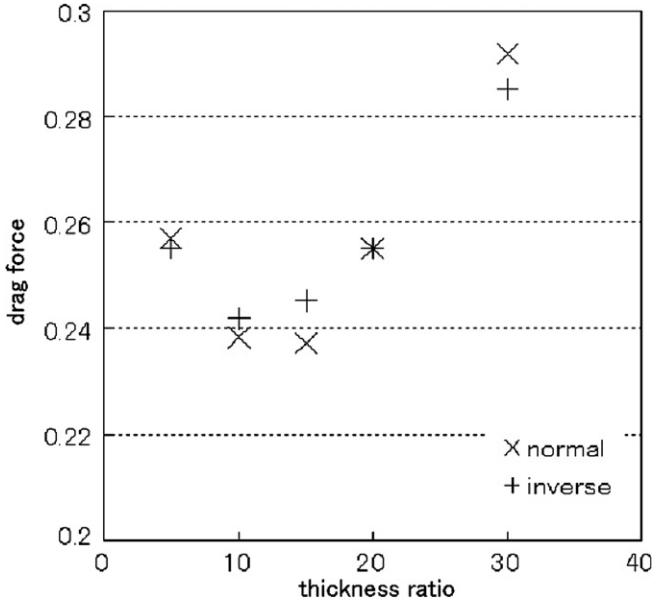

Fig. 10. Drag forces (amplified).

5. Conclusion

In this study, the shape optimization in the incompressible viscous flow is presented based on the finite element method originated by the authors group. The used mesh is the triangular elements. To obtain the smooth gradient the smoothing is introduced. The adjoint equation is derived from the stationary condition of the performance function. As the control variable, coordinate of the body shape is utilized. The weighted gradient method is used for the minimization algorithm because the stable computation secures starting from the wide-range of the initial condition. The operation of changing the body shape starting from a circular cylinder as an initial body shape. Based on the present procedure, it is not necessary to introduce the re-meshing to obtain the smoothed gradient.

The front-edged and rear-round type shape is obtained as the final shape, of which drag force is reduced by 66.5% comparing with the initial circular cylinder. This paper detected out that the Reynolds number 250 flow seems critical at which the shape of the minimum drag force changes from the front-edged shape to front-round shape. This fact is very important not only in the sense of academic work but also of the practical work. For instance the shape of the champion of the man-powered airplane race shows the front-edged and rear-round shape.

Acknowledgements

Authors are very much grateful to professor Mikio Hino, emeritus professor of Chuo University for his kind encouragements and helpful discussions.

References

[1] O. Pironneau, On optimum profiles in Stokes flow, J. Fluid Mech. 59 (1973), Part 1.
[2] O. Pironneau, On optimum shape design in fluid mechanics, J. Fluid Mech. 64 (1974), Part 1.
[3] B. He, O. Ghattas, J.F. Antaki, Computational strategies for shape optimization of time-dependent Navier–Stokes flows, Technical Report CMU-CML-97-102, 1997.
[4] A. Maruoka, M. Kawahara, Optimal control in Navier–Stokes equation, Int. J. Comput. Fluid Dyn. 9 (1998) 313–322.
[5] J. Matsumoto, T. Umetsu, M. Kawahara, Incompressible viscous flow analysis and adaptive finite element method using linear bubble function, J. Appl. Mech. 2 (1999) 223–232.
[6] J. Matsumoto, M. Kawahara, Stable shape identification for fluid-structure interaction problem using MINI element, J. Appl. Mech. 3 (2000) 263–274.
[7] H. Okumura, M. Kawahara, Shape optimization of body located in incompressible Navier–Stokes flow based on optimal control theory, CMES 1 (2) (2000) 71–77.
[8] B. Mohamadi, O. Pironneau, Applied Shape Optimization for Fluids, Oxford University Press, 2001.
[9] A. Jameson, Aerodynamic shape optimization using the adjoint method, Lecture at the Von Karman Institute, Brussels, 2003.
[10] K. Leoviriyakit, A. Jameson, Aerodynamic shape optimization of wings including platform variations, in: Proc. of 44th Aero/Astro Industrial Affiliates Meeting, Stanford, April 29–30, 2003.
[11] Y. Ogawa, M. Kawahara, Shape optimization of a body located in incompressible viscous flow based on optimal control theory, Int. J. Comput. Fluid Dyn. 17 (4) (2003) 243–251.
[12] H. Yagi, M. Kawahara, Shape optimization of a body located in low Reynolds number flow, Int. J. Numer. Methods Fluids 48 (2005) 819–833.
[13] E. Katamine, H. Azegami, T. Tsubata, S. Itoh, Solution to shape optimization problems of viscous flow fields, Int. J. Comput. Fluid Dyn. 19 (1) (2005) 45–51.
[14] T.J.R. Hughes, L.P. Franca, M. Balestra, A new finite element formulation for computational fluid dynamics: V. Circumventing the Babuska–Brezzi condition: A stable Petrov–Galerkin formulation of the Stokes problem accommodating equal order interpolation, Comput. Methods Appl. Mech. Engrg. 59 (1986) 85–99.